Facile Anionic Synthesis of Well-Defined Block Copolymers with Pendent Triphenylamine and Ethynylpyridine for Nonvolatile Memory Device Applications with High Performances

Beom-Goo Kang,[1] Sunghoon Song,[2] Byungjin Cho,[3] Nam-Goo Kang,[1] Myung-Jin Kim,[1] Takhee Lee,[4] Jae-Suk Lee[1]

[1]School of Materials Science and Engineering, Department of Nanobio Materials and Electronics, Gwangju Institute of Science and Technology (GIST), 123 Cheomdan-gwagiro (Oryong-dong), Buk-gu, Gwangju 500-712, Korea
[2]Samsung Electronics, San #24 Nongseo-dong, Giheung-gu, Yongin-si, Gyeonggi-do 446-711, Korea
[3]Advanced Functional Thin Films Department, Korea Institute of Materials Science, Changwon 641-831, Korea
[4]Department of Physics and Astronomy, Seoul National University, Seoul 151-747, Korea
Correspondence to: J.-S. Lee (E-mail: jslee@gist.ac.kr)

Received 6 January 2014; accepted 30 May 2014; published online 20 June 2014
DOI: 10.1002/pola.27278

ABSTRACT: The sequential block copolymerization of 4,4′-vinylphenyl-*N*,*N*-bis(4-*tert*-butylphenyl)benzenamine (**A**) with 2-(2-(4-vinylphenyl)ethynyl)pyridine (**B**) was simply carried out using only potassium naphthalenide (K-Naph) as an initiator without any additives in tetrahydrofuran (THF) at −78 °C. The well-defined functional block copolymers containing **A** block as an electron donor and **B** block as a weak electron acceptor had predictable molecular weights (M_n = 8,800–14,500 g/mol) and narrow molecular weight distributions (M_w/M_n = 1.09–1.10). The bicontinuous microphase-separated film morphology of the precisely synthesized poly(**B**-*b*-**A**-*b*-**B**) (P**BAB**) with 0.71 of $f_{poly(A)}$, formed by thermal annealing at 230 °C for 9 h, was expected to be a potential active layer for nonvolatile memory device applications. Indium tin oxide (ITO)/P**BAB**/aluminum (Al) memory devices with an 8 × 8 cross-bar array structure exhibited nonvolatile resistive switching characteristics. The memory devices showed reliable memory performance in terms of ON/OFF ratios of ~10^4, endurance cycles and retention time, and statistical data with regard to cumulative probability of the switching currents and threshold voltage distribution. Filamentary conduction mechanism was proposed to explain the switching of P**BAB**-based memory devices. © 2014 Wiley Periodicals, Inc. J. Polym. Sci., Part A: Polym. Chem. **2014**, *52*, 2625–2632

KEYWORDS: anionic polymerization; electron donor–acceptor; filamentary conduction; functional block copolymer; non-volatile memory

INTRODUCTION Electron donor–acceptor (D–A) polymers have been widely used for polymer memory device applications due to their advantages such as low cost solution processing and flexibility.[1–9] Among the reported D–A polymers, nonconjugated polymers with pendent D–A have been in particular considered to be suitable materials for investigating the effects of pendent D–A ratios on the electrical memory properties. For these memory materials with different pendent D–A ratios, advanced polymerization method has been reported during the past 2 years. Chen group especially developed to synthesize nonconjugated random copolymers with pendent electron-donating carbazole or triphenylamine moieties and electron-accepting oxadiazole moieties through nitroxide-mediated free radical polymerization (NMRP) technique for memory device applications.[3,4] They demonstrated that the memory switching characteristics could be tuned by changing pendent D–A ratios.

Recently, it has been also reported that the morphologies of block copolymers with pendent D–A significantly influence memory characteristics.[7,10] However, it is generally difficult for the random copolymers mentioned above to manipulate the memory switching characteristics by controlling morphologies because it is almost impossible to achieve a thoroughly controlled molecular weight distribution from the random copolymers. Accordingly, a different polymerization method, which can precisely synthesize the block copolymers with pendent D–A, is required to observe exactly the effects of the morphologies on the memory switching characteristics.

Additional Supporting Information may be found in the online version of this article.

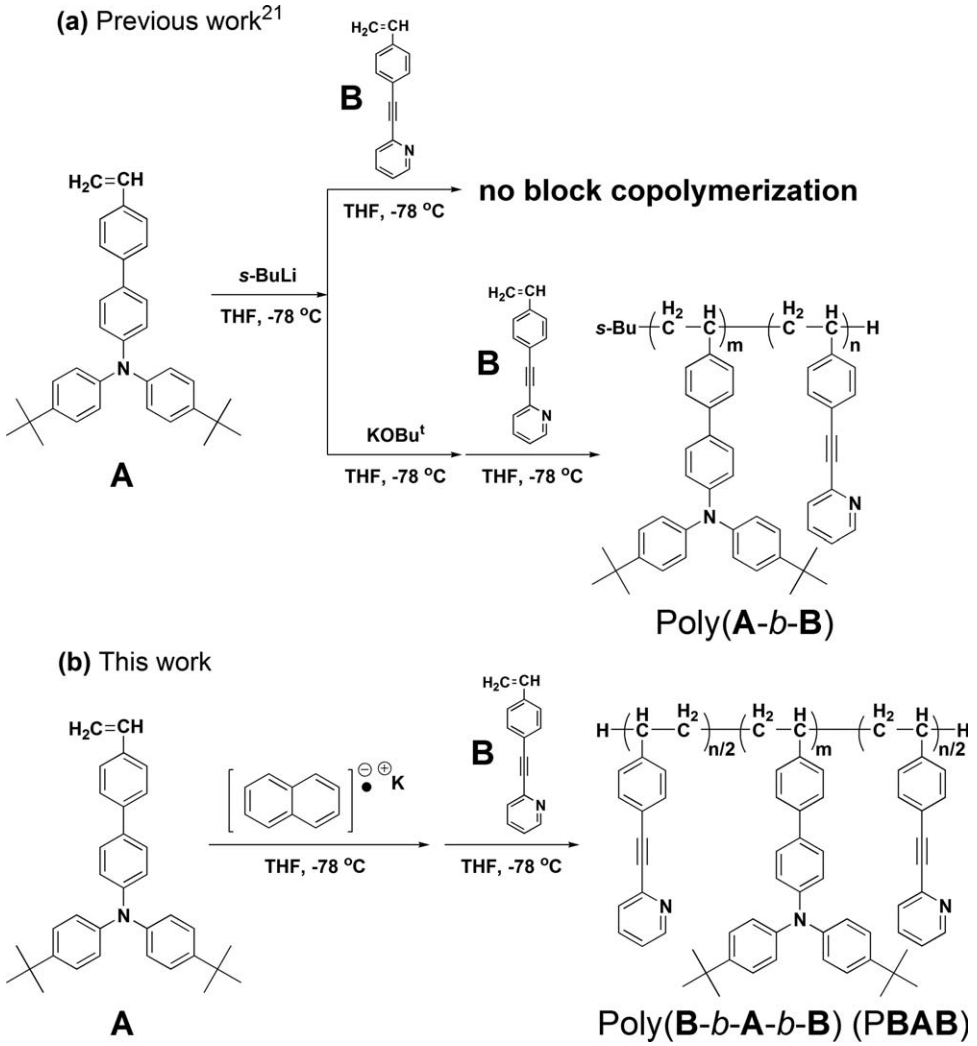

SCHEME 1 Synthetic route of (a) poly(**A**-*b*-**B**) and (b) P**BAB**.

It has been well known that anionic polymerization is the most established synthetic method to prepare the block copolymers with precise molecular structures.[11–15] Nevertheless, from a synthetic point of view, the vinyl monomers containing D or A moieties in functional groups are problematic in anionic systems because D or A mostly possess heteroatoms such as nitrogen and oxygen. In general, undesirable side reactions take place in anionic polymerization of the vinyl monomers with heteroatom-containing functional groups due to the incompatibility of the functional groups with carbanion species such as anionic initiators and propagating chain-end anions.[12] To overcome these problems, in our group, we have been studying the living anionic polymerization and block copolymerization of styrene derivatives containing pyridine, triphenylamine and carbazole moieties, and optimally established their synthetic conditions.[16–20]

In particular, we recently reported that in contrast to the block copolymerization of 4,4′-vinylphenyl-*N,N*-bis(4-*tert*-butylphenyl)benzenamine (**A**) with 2-(2-(4-vinylphenyl)ethynyl)pyridine (**B**) using *sec*-butyllithium (*s*-BuLi) in the absence of potassium *tert*-butoxide ($KOBu^t$), the block copolymerization was successfully performed by adding $KOBu^t$ prior to polymerization of **B** [Scheme 1(a)].[21] It was suggested that an exchange of countercation from Li^+ to K^+ through using excess $KOBu^t$ affects the polymerization behavior of **B**. The well-defined block copolymers with pendent triphenylamine and ethynylpyridine were quantitatively prepared by the less reactive ion pair (poly(**A**)$^-K^+$) formed by the addition of $KOBu^t$. Therefore, such an effect of countercation on anionic polymerization behavior allowed us to further search for facile anionic block copolymerization conditions.

In this paper, we report on the facile anionic synthesis and memory device characteristics of the well-defined block copolymers with pendent triphenylamine and ethynylpyridine. The functional block copolymers containing **A** block as an electron donor and **B** block as a weak electron acceptor were simply synthesized by using only K-Naph initiator with K^+ countercation in the absence of any additives. The memory devices fabricated with the resulting block copolymer showing bicontinuous microphase-separated structure exhibited high

TABLE 1 Block Copolymerization of **A** with **B** using K-Naph in THF at −78 °C.[a]

Run	K-Naph (mmol)	Monomer		Block Copolymer (Homopolymer) $M_n \times 10^{-3}$			
		1st (mmol)	2nd (mmol)	calcd[b]	obsd[c]	M_w/M_n[d]	$f_{poly(A)}$[e]
1	0.103	**A**, 1.33	**B**, 0.482	14.2 (11.9)	14.5 (12.3)	1.09 (1.08)	0.71
2	0.070	**A**, 0.470	**B**, 0.556	9.7 (6.2)	8.8 (5.6)	1.10 (1.06)	0.44
3	0.121	**A**, 0.546	**B**, 1.66	10.0 (4.1)	10.8 (4.4)	1.10 (1.05)	0.23

[a] Polymer yield was quantitative. Polymerization times were total 4.5, 0.5 h for **A** and 4 h for **B**.
[b] M_n (calcd) = (molecular weight of monomer) × [monomer] × 2/[initiator].
[c] M_n of the block copolymer was determined using M_n of the homopolymer and the molar ratio of each block estimated by ^{1}H NMR.
[d] M_w/M_n was determined using SEC calibration with polystyrene standards in a THF solution containing 2% triethylamine as the eluent at 40 °C.
[e] Determined by ^{1}H NMR.

performances with regard to nonvolatile memory characteristics. Based on our previous memory research that block copolymer system possessing well-ordered microphase-separated morphology shows nonvolatile resistive switching characteristics, filamentary conduction mechanism was proposed to explain the switching behavior of memory devices.[7]

EXPERIMENTAL

Materials

4,4′-Vinylphenyl-*N*,*N*-bis(4-*tert*-butylphenyl)benzenamine (**A**), 2-(2-(4-vinylphenyl)ethynyl)pyridine (**B**) and K-Naph were prepared according to previously published papers.[17,18,22] The monomers and K-Naph were diluted with THF and divided into ampules with break-seals on a vacuum line. The ampules were stored at −30 °C prior to polymerization.

Measurements

^{1}H NMR spectra were obtained using $CDCl_3$ as a solvent at 25 °C (JEOL JNM-ECX400). The chemical shifts are in reference to tetramethylsilane (TMS) at 0 ppm. FT-IR spectroscopy was carried out from 4000 to 400 cm^{-1} using KBr pellets (Perkins-Elmer Spectrum 2000). The polymers were characterized by size exclusion chromatography (SEC, Waters M77251, M510). The molecular weight distributions of the polymers were determined using SEC calibration with polystyrene standards (American Polymer Standards Corp.) in a THF solution containing 2% triethylamine as the eluent at 40 °C. The thermal properties were investigated with thermogravimetric analysis (TA Instrument, TGA-Q50) and differential scanning calorimetry (TA Instrument, DSC-Q20) at a heating rate of 10 °C/min under nitrogen. UV–vis absorption spectra were obtained using an Agilent 8453 UV–vis spectrophotometer. The morphologies of the polymer were characterized with a field emission transmission electron microscope (FE-TEM, JEOL JEM-2100F).

Block Copolymerization of A with B Using K-Naph

The first-stage polymerization of **A** was performed with K-Naph in THF at −78 °C for 0.5 h in an all-glass apparatus equipped with break-seals under high vacuum. After a portion of the living poly(**A**) was sampled to characterize, **B** was added to the living poly(**A**) solution, and the reaction was continued at −78 °C for 4 h. The terminated solutions were poured into a large amount of methanol to obtain poly(**A**) and P**BAB**. The resulting block copolymer was characterized by SEC and ^{1}H NMR. P**BAB** [M_n(obsd) = 14,500 g/mol, M_w/M_n = 1.09 (Table 1, run 1)]. ^{1}H NMR (400 MHz, $CDCl_3$): δ = 1.10–2.18 (CH_2–CH and *tert*-butyl), 6.30–7.62 (phenyl and pyridine). 8.52 (CH═N of pyridine).

Fabrication and Characterization of Memory Device

Figure 4 shows the fabrication process of memory devices with a P**BAB** active layer. ITO/P**BAB**/Al devices with an 8 × 8 cross-bar array structure were fabricated. 120 nm thick ITO on a glass substrate was cleaned by the typical ultrasonic cleaning process using de-ionized water, acetone and isopropyl alcohol for 10 min, respectively [Fig. 4(a)]. The ITO used as a bottom electrode was patterned with eight lines by conventional photolithography and an etching process [Fig. 4(b)]. The P**BAB** dissolved in chlorobenzene (1.0 wt %) was spin-coated on to the patterned ITO electrodes at 2000 rpm for 40 s and then the polymer film was annealed at 230 °C for 9 h to remove residual solvent and promote microphase separation [Fig. 4(c)]. The thickness of the P**BAB** active layer was measured to be 47 nm from the cross-sectional transmission electron microscopy (TEM) analysis. In order to form top electrodes, 41 nm thick Al layer was deposited by thermal evaporator with the deposition rate of 5 Å/s at a pressure of $\sim 10^{-7}$ Torr [Fig. 4(d)]. From TEM energy dispersive X-ray spectroscopy (EDX) analysis, it was confirmed that each layer of memory device was well separated. All electrical measurements were performed using a semiconductor characterization system (Keithley 4200 SCS) at room temperature in a N_2-filled glove box.

RESULTS AND DISCUSSION

Facile Anionic Synthesis of Block Copolymer

From the synthetic viewpoint, the successful achievement of living anionic polymerization of **A** using *s*-BuLi as an initiator in THF at –78 °C, proved in our previous study,[18] enables

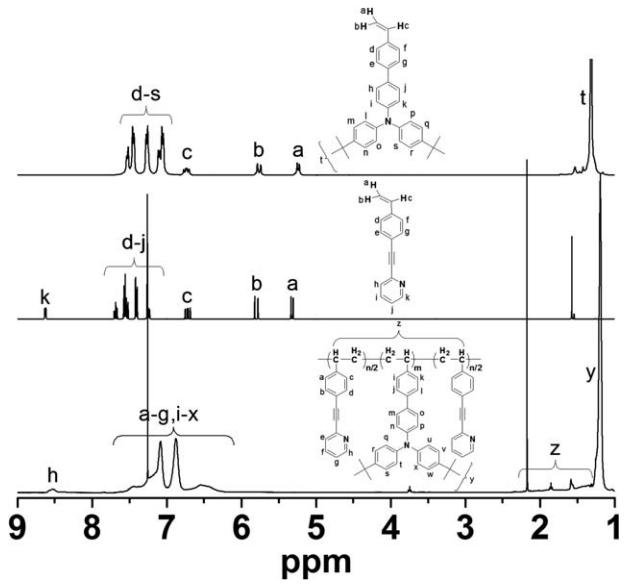

FIGURE 1 ^{1}H NMR spectra of **A**, **B** and P**BAB** in $CDCl_3$.

the well-defined block copolymers with pendent D–A to be synthesized by the sequential block copolymerization. **B** was selected as comonomer with electron-accepting pyridine moieties. However, the block copolymerization of **A** with **B** using *s*-BuLi was not performed due to side reactions during the polymerization of **B**. In contrast, the well-defined block copolymers (poly(**A**-*b*-**B**)) were successfully synthesized in the presence of $KOBu^t$ [Scheme 1(a)]. From these polymerization results, it was demonstrated that the block copolymerization of **A** with **B** using *s*-BuLi as an initiator in THF at -78 °C is entirely dependent on the addition of $KOBu^t$ prior to polymerization of **B**.[21] It is believed that the polymerization results improved by using excess $KOBu^t$ may possibly be due to the change in the countercation from Li^+ to K^+ and the suppression of ion dissociation by the salt common effect, resulting in less reactive ion pair (poly(**A**)$^-K^+$) in polar THF media, which suppresses the undesirable side reactions in the polymerization of **B**. These findings allowed us to further search for facile synthetic conditions for preparing the well-defined functional block copolymers with pendent triphenylamine and ethynylpyridine.

Based on the precise synthesis of poly(**A**-*b*-**B**), the block copolymerization of **A** with **B** was carried out by using only K-Naph initiator with K^+ countercation in THF at -78 °C in the absence of any additives, as shown in Scheme 1(b). When **A** was added to the initiator solution, the color of polymerization solution became deep violet. This color turned deep blue immediately after adding **B** into the living poly(**A**) solution. These distinct colors were identical to those observed in block copolymerization of **A** with **B** using *s*-BuLi in the presence of $KOBu^t$, and obviously maintained during polymerization (Fig. S1 in the Supporting Information).

As shown in Figure 1, ^{1}H NMR spectra of **A, B**, and P**BAB** indicate that polymerization proceeded exclusively. The peaks of vinyl group of the monomers disappeared after polymerization, whereas the broad peak of the main polymer chain (1.10–2.18 ppm), and the broad characteristic singlet of both *tert*-butyl (1.19 ppm) and pyridine group (8.52 ppm) were observed, respectively. In addition to ^{1}H NMR results, the characteristic C≡C band of **B** block was found at 2221 cm^{-1} in FT-IR spectrum of the resulting block copolymer (Fig. S2 in the Supporting Information). As summarized in Table 1, the well-defined block copolymers with predictable M_n (8,800–14,500 g/mol) and narrow M_w/M_n (1.09–1.10) were precisely synthesized. The observed M_n values of P**BAB** agreed well with the calculated ones based on monomer to initiator ratios, and all SEC curves of P**BAB** were unimodal and narrow. For example, the block copolymerization proceeded quantitatively with K-Naph in THF at -78 °C for 4.5 h (Table 1, run 1). The observed M_n (14,500 g/mol) was in well accordance with the calculated M_n (14,200 g/mol). In addition, narrow SEC curve of P**BAB** (M_w/M_n = 1.09) was completely shifted from elution volume of poly(**A**) toward a higher M_n region [Fig. 2]. These indicate that the block copolymerization of **A** with **B** can be simply performed by using only K-Naph initiator without any additives, suggesting that polymerization process for preparing the well-defined block copolymers with pendent triphenylamine and ethynylpyridine is simplified, as compared to the previously reported synthetic method using *s*-BuLi and $KOBu^t$. From the previous and present results of the block copolymerization of **A** with **B**, it is verified that the chain-end anion of poly(**A**), associated with K^+ countercation, can successfully polymerize **B** without occurrence of any side reactions, indicating that the countercation significantly affects the block copolymerization of **A** with **B**.

Characterizations of Block Copolymer

The our previous study on relationship between film morphologies and electrical properties of block copolymer-based nonvolatile memory device demonstrated that the devices based on block copolymer system showing well-ordered microphase-separated structure exhibit nonvolatile resistive switching characteristics with excellent memory performances.[7] Based on this research, we attempted to observe ordered microphase-separated structures from three P**BAB**

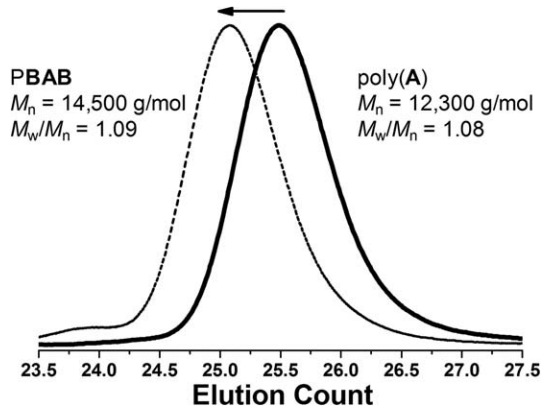

FIGURE 2 SEC curves of poly(**A**) and P**BAB** (Table 1, run 1).

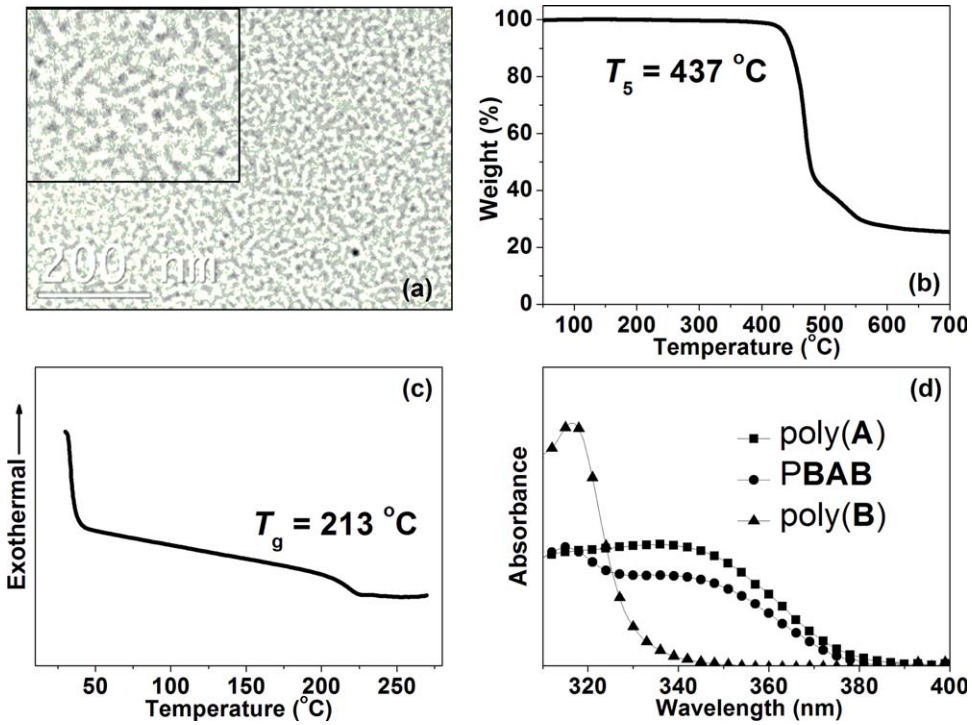

FIGURE 3 (a) TEM image of P**BAB**71 annealed at 230 °C for 9 h. (b) TGA and (c) DSC thermograms of P**BAB**71 under nitrogen with a heating rate of 10 °C/min. (d) UV–vis absorption spectra of poly(**A**), P**BAB**71 and poly(**B**) in thin film state. [Color figure can be viewed in the online issue, which is available at wileyonlinelibrary.com.]

with different block ratios synthesized in this study [Table 1]. Among them, bicontinuous microphase-separated morphology of P**BAB** with 0.71 of $f_{\text{poly(A)}}$ (Table 1, run 1) was observed by thermal annealing. From here, we denote the P**BAB** with 0.71 of $f_{\text{poly(A)}}$ as P**BAB**71 for simplicity. The polymer solution in chlorobenzene was drop-casted onto the carbon-coated copper grid and annealed at 230 °C for 9 h to satisfactorily promote microphase separation. The iodine (I_2) was subsequently used for 10 h to stain the annealed sample. The bicontinuous microphase-separated morphology of the annealed block copolymer was confirmed by TEM, as shown in Figure 3(a). In TEM image of block copolymer nanostructure, **A** block is shown as white, in contrast, **B** block is shown as black because **B** block was stained by I_2 vapor. The solubility test showed that P**BAB**71 was soluble in chloroform, THF, toluene, 1,2-dichloroethane, and chlorobenzene. In particular, the polymer solution dissolved in chlorobenzene was well spin-coated on the substrate. The thermal properties of P**BAB**71 were determined by thermogravimetric analysis (TGA) and differential scanning calorimetry (DSC) under nitrogen. The values of the 5% weight loss temperature (T_5) and the glass transition temperature (T_g) of the polymer were measured to be 437 and 213 °C, respectively [Fig. 3(b,c)]. Figure 3(d) shows UV–vis absorption spectra of poly(**A**), P**BAB**71 and poly(**B**) in thin film state. The absorption maxima (λ_{max}) of poly(**A**) and poly(**B**) were observed at 336 and 317 nm, respectively, due to the π–π^* transition of the triphenylamine moiety in poly(**A**) and the aromatic ring in poly(**B**). The absorption band of P**BAB**71 was well matched with combination of the absorption band of poly(**A**) and poly(**B**). The maximum peaks of P**BAB**71 ascribed to the π–π^* transition of **A** block and **B** block were found at 334 and 315 nm, respectively. From the results of various characterizations, it was expected that bicontinuous microphase-separated structure induced by thermal annealing, good film-forming properties and excellent thermal properties allow the P**BAB**71 to be a potential active layer for nonvolatile memory devices with high performances.

Memory Device Performances

Figure 5(a) shows the schematic illustration of 8 × 8 array-type memory device consisting of ITO/P**BAB**71/Al layers. The details of the device fabrication are explained and illustrated in the Experimental Section and Figure 4. All the memory cells (a total of 8 × 8 = 64) were electrically investigated to evaluate their memory characteristics. The representative current–voltage (I–V) switching characteristic from the selected cell of the memory device is shown in Figure 5(b). First, when double sweep measurement from 0 to 8 V was performed, initial high resistance state (HRS, OFF state) of the memory device was abruptly turned into low resistance state (LRS, ON state) at a threshold voltage ($V_{th} \sim 3.1$ V) and then the ON state was retained even after the applied voltage returned to 0 V, indicating nonvolatile memory characteristics. When the device was under the single sweeping mode from 0 to 15 V, the device followed the track of the

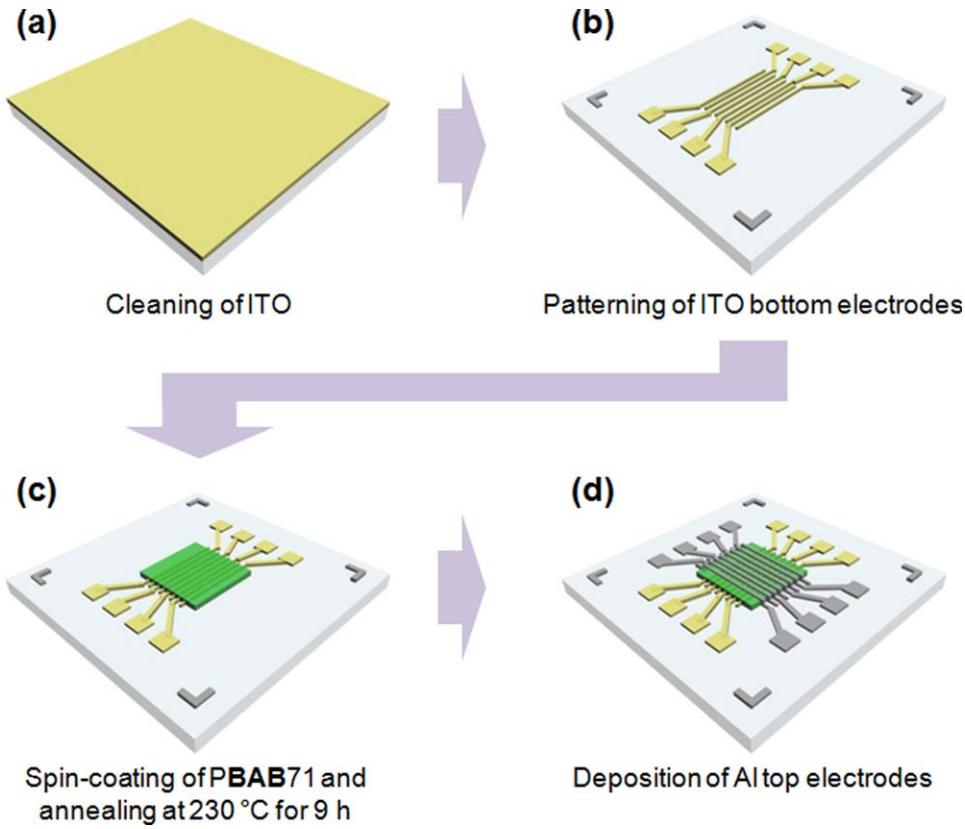

FIGURE 4 Schematic illustration of the fabrication processes of ITO/P**BAB**71/Al device with an 8 × 8 array structure. [Color figure can be viewed in the online issue, which is available at wileyonlinelibrary.com.]

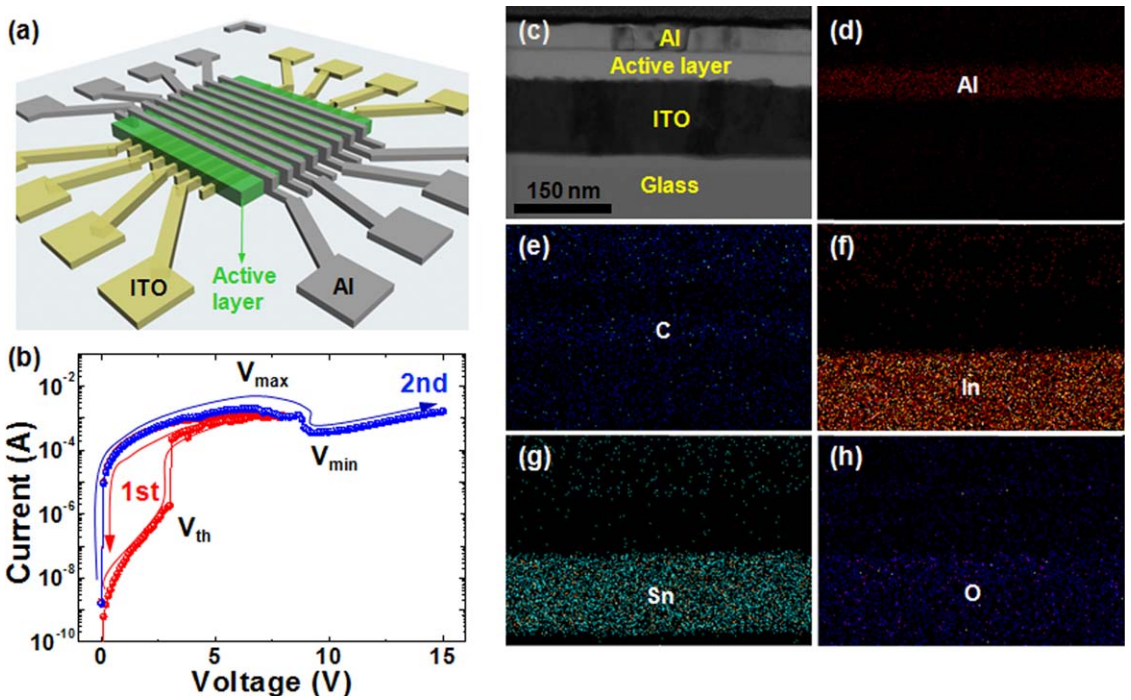

FIGURE 5 (a) The schematic illustration of 8 × 8 array-type memory device consisting of ITO/P**BAB**71/Al layers. (b) The representative current–voltage (I–V) switching characteristic of the memory device. (c) Cross-sectional TEM image of the memory device. TEM EDX mapping image of (d) aluminum, (e) carbon, (f) indium, (g) tin and (h) oxygen. [Color figure can be viewed in the online issue, which is available at wileyonlinelibrary.com.]

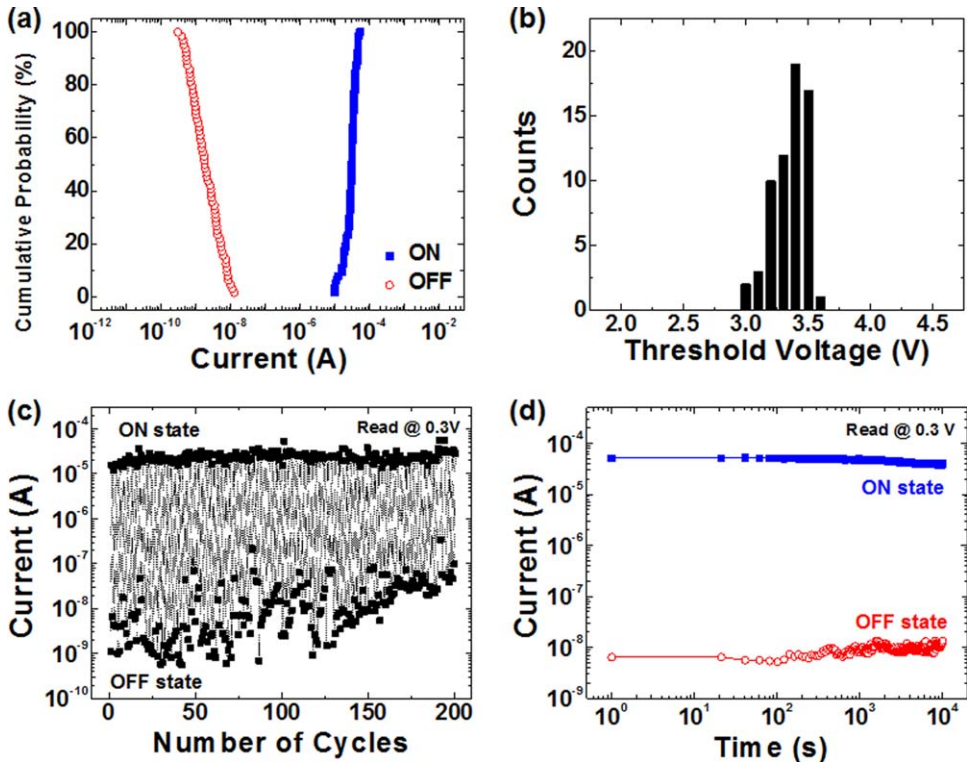

FIGURE 6 (a) Cumulative probability of ON and OFF states and (b) statistical distributions of the threshold voltages of all the operative memory cells. (c) The dc sweep endurance characteristics and (d) retention time of a single cell. [Color figure can be viewed in the online issue, which is available at wileyonlinelibrary.com.]

ON state and then it was turned off at 9.3 V. Consequently, ON/OFF ratio of $\sim 10^4$ was obtained. The typical unipolar switching behavior of our memory device was also completely reversible (not shown here). Figure 5(c) shows a cross-sectional TEM image of the memory device consisting of P**BAB**71 (47 nm) active layer sandwiched between Al (41 nm) and ITO (120 nm) electrodes. The cross-sectional TEM image with thickness of each layer is shown in Figure S3 in the Supporting Information. In addition, the element distribution of aluminum (Al), carbon (C), indium (In), tin (Sn) and oxygen (O) in each layer of the memory device was investigated by TEM EDX [Fig. 5(d–h)]. In particular, it was shown that there is no penetration of Al elements into the active layer; unintentional penetration of Al elements can create unwanted high conductive paths and cause electrical short of the devices.

The charge transfer effect between triphenylamine (donor) and pyridine (weak acceptor) on resistive switching properties of our memory devices is likely to be negligible because the strong insulating characteristic of the pyridine homopolymer was proved experimentally in our previous study.[7] Also, it is excluded that top metal (Al) diffusion into P**BAB**71 active layer affects the resistive switching because both cross-sectional TEM and TEM EDX mapping images showed that each layer of the devices is well separated. For the possible mechanism for our memory devices, we now believe that conductive paths mainly consisting of conducting triphenylamine units might be formed or ruptured by an electrical field. Such a resistive switching has often been described by filamentary switching model.[7,23,24] In particular, based on our previous study, it can be proposed that filamentary paths are most favorably grown and then easily broke up in bicontinuous microphase-separated structure of P**BAB**71, resulting in a reversible resistance change.[7]

The statistical data of the switching characteristics of all the operative memory cells are shown in Figure 6. The memory exhibited 100% device yield; 64 cells out of 64 were operative as a resistive switching memory. As shown in Figure 6(a), ON and OFF states of all the operative cells were cumulatively plotted. Although the distribution of the OFF current values seems to be relatively wider than that of the ON current values, the important point of this data is that the ON and OFF current is consistently separated by more than three orders of magnitude. Moreover, the statistical distributions of the threshold voltages of the operative cells show that the transition from the OFF state to the ON state occurs at voltages in the very narrow range of 3.0–3.6 V [Fig. 6(b)]. Thus, such a small variation in the threshold voltages would significantly reduce a failure in writing the memory cells.

The endurance and retention test were carried out to evaluate the performance of memory device. Firstly, to investigate endurance, we applied a repetitive dc voltage to the memory

cells. The ON/OFF current ratios of over $\sim 10^3$ were maintained without any significant electrical degradation during 200 sweep cycles [Fig. 6(c)]. Next, the retention capability of each state was also examined. As shown in Figure 6(d), the memory device maintained the ON/OFF current ratios of over $\sim 10^4$ and showed stable retention properties during a long retention period of 10^4 s, indicating excellent nonvolatile memory characteristic.

CONCLUSIONS

We observed that the successful anionic block copolymerization of **A** with **B** was simply performed using only K-Naph initiator with K^+ countercation in the absence of any additives to afford the well-defined block copolymer with pendent triphenylamine and ethynylpyridine (P**BAB**). The memory devices fabricated using the block copolymer with bicontinuous microphase-separated morphology showed excellent nonvolatile memory performances. Filamentary conduction mechanism was suggested to explain the switching behavior of P**BAB**-based memory devices. The memory showed 100% device yield (64 cells), narrow distributions of threshold voltages (3.0–3.6 V), good switching endurance ($\sim$200 cycles) and retention times ($\sim 10^4$ s) with ON/OFF current ratios of $\sim 10^4$. For the further work, it is expected that P**BAB** will potentially be able to be used in the three-dimensionally stackable polymer memory devices because the ethynyl groups in **B** block are crosslinked by thermal treatment (Fig. S4 in the Supporting Information).[21,25]

ACKNOWLEDGMENTS

This work was supported by the GIST-Caltech Research Institute Program at GIST, the World-Class University Program through the National Research Foundation of Korea (R31-10026), and the Gyeongsangnam, Changwon Science Research Park Project of the Grant of the Korean Ministry of Science, ICT and Future Planning.

REFERENCES AND NOTES

1 Q.-D. Ling, D.-J. Liaw, C. Zhu, D. S.-H. Chan, E.-T. Kang, K.-G. Neoh, *Prog. Polym. Sci.* **2008**, *33*, 917–1012.

2 X.-D. Zhuang, Y. Chen, G. Liu, B. Zhang, K.-G. Neoh, E.-T. Kang, C.-X. Zhu, Y.-X. Li, L.-J. Niu, *Adv. Funct. Mater.* **2010**, *20*, 2916–2922.

3 Y.-K. Fang, C.-L. Liu, W.-C. Chen, *J. Mater. Chem.* **2011**, *21*, 4778–4785.

4 Y.-K. Fang, C.-L. Liu, G.-Y. Yang, P.-C. Chen, W.-C. Chen, *Macromolecules* **2011**, *44*, 2604–2612.

5 C.-L. Liu, W.-C. Chen, *Polym. Chem.* **2011**, *2*, 2169–2174.

6 T. Kurosawa, Y.-C. Lai, T. Higashihara, M. Ueda, C.-L. Liu, W.-C. Chen, *Macromolecules* **2012**, *45*, 4556–4563.

7 N.-G. Kang, B. Cho, B.-G. Kang, S. Song, T. Lee, J.-S. Lee, *Adv. Mater.* **2012**, *24*, 385–390.

8 S. G. Hahm, N.-G. Kang, W. Kwon, K. Kim, Y.-G. Ko, S. Ahn, B.-G. Kang, T. Chang, J.-S. Lee, M. Ree, *Adv. Mater.* **2012**, *24*, 1062–1066.

9 H.-C. Wu, C.-L. Liu, W.-C. Chen, *Polym. Chem.* **2013**, *4*, 5261–5269.

10 B. Ahn, D. M. Kim, J.-C. Hsu, Y.-G. Ko, T. J. Shin, J. Kim, W.-C. Chen, M. Ree, *ACS Macro Lett.* **2013**, *2*, 555.

11 N. Hadjichristidis, M. Pitsikalis, S. Pispas, H. Iatrou, *Chem. Rev.* **2001**, *101*, 3747–3792.

12 A. Hirao, S. Loykulnant, T. Ishizone, *Prog. Polym. Sci.* **2002**, *27*, 1399.

13 D. Uhrig, J. W. Mays, *J. Polym. Sci. Part A: Polym. Chem.* **2005**, *43*, 6179–6222.

14 D. Uhrig, J. W. Mays, *Polym. Chem.* **2011**, *2*, 69–76.

15 A. Hirao, K. Murano, T. Oie, M. Uematsu, R. Goseki, Y. Matsuo, *Polym. Chem.* **2011**, *2*, 1219–1233.

16 N.-G. Kang, M. Changez, J.-S. Lee, *Macromolecules* **2007**, *40*, 8553–8559.

17 B.-G. Kang, N.-G. Kang, J.-S. Lee, *J. Polym. Sci. Part A: Polym. Chem.* **2011**, *49*, 5199–5209.

18 B.-G. Kang, N.-G. Kang, J.-S. Lee, *Macromolecules* **2010**, *43*, 8400–8408.

19 Y.-S. Cho, C.-S. Ihn, S.-W. Kim, J.-S. Lee, *Polymer* **2001**, *42*, 7611–7616.

20 N.-G. Kang, Y.-H. Hur, M. Changez, B.-G. Kang, Y.-G. Yu, J.-S. Lee, *Polymer* **2013**, *54*, 5615–5625.

21 B.-G. Kang, Y.-G. Yu, N.-G. Kang, J.-S. Lee, *J. Polym. Sci. Part A: Polym. Chem.* **2013**, *51*, 4233–4239.

22 K. Tsuda, T. Ishizone, A. Hirao, S. Nakahama, T. Kakuchi, K. Yokota, *Macromolecules* **1993**, *26*, 6985–6991.

23 M. Cölle, M. Büchel, D. M. de Leeuw, *Org. Electron.* **2006**, *7*, 305.

24 G. Dearnaley, D. V. Morgan, A. M. Stoneham, *J. Non-Cryst. Solids* **1970**, *4*, 593–612.

25 B.-G. Kang, H. Kang, N.-G. Kang, C.-L. Lee, K. Lee, J.-S. Lee, *Polym. Chem.* **2013**, *4*, 969–977.